Prospects for Higgs coupling measurements in SUSY with radiatively-driven naturalness

Kyu Jung Bae, Howard Baer, Natsumi Nagata, and Hasan Serce

Phys. Rev. D **92**, 035006 — Published 14 August 2015

DOI: 10.1103/PhysRevD.92.035006

OU-HEP-150430
FTPI-MINN-15/23
IPMU15-0070

Prospects for Higgs coupling measurements in SUSY with radiatively-driven naturalness

Kyu Jung Bae[1*], Howard Baer[1†], Natsumi Nagata[2,3‡] and Hasan Serce[1§]

[1] *Dept. of Physics and Astronomy, University of Oklahoma, Norman, OK 73019, USA*
[2] *William I. Fine Theoretical Physics Institute, School of Physics and Astronomy, University of Minnesota, Minneapolis, MN 55455, USA*
[3] *Kavli IPMU (WPI), UTIAS, University of Tokyo, Kashiwa, Chiba 277-8583, Japan*

Abstract

In the post-LHC8 world– where a Standard Model-like Higgs boson has been established but there is no sign of supersymmetry (SUSY)– the detailed profiling of the Higgs boson properties has emerged as an important road towards discovery of new physics. We present calculations of the expected deviations in Higgs boson couplings $\kappa_{\tau,b}$, κ_t, $\kappa_{W,Z}$, κ_g and κ_γ versus the naturalness measure $\Delta_{\rm EW}$. Low values of $\Delta_{\rm EW} \sim 10-30$ give rise to a natural Little Hierarchy characterized by light higgsinos with a mass of $\mu \sim m_Z$ while top squarks are highly mixed but lie in the several TeV range. For such models with radiatively-driven naturalness, one expects the Higgs boson h to look very SM-like although deviations can occur. The more promising road to SUSY discovery requires direct higgsino pair production at a high energy e^+e^- collider operating with the center-of-mass energy $\sqrt{s} > 2\mu \sim \sqrt{2\Delta_{\rm EW}}m_Z$.

*Email: bae@nhn.ou.edu
†Email: baer@nhn.ou.edu
‡Email: natsumi.nagata@ipmu.jp
§Email: serce@ou.edu

1 Introduction

The recent discovery of a Standard Model (SM)-like Higgs boson [1,2] with mass $m_h = 125.09 \pm 0.24$ GeV [3] (ATLAS/CMS combined values) is a triumph of contemporary physics in that it provides the first hard evidence for the existence of fundamental scalar fields. Theoretically, such spinless fields are hard to comprehend due to unstable quadratic quantum corrections to their mass value [4]. If nature is supersymmetric (SUSY), then the unwanted divergences are cancelled to all orders in perturbation theory thus allowing for a naturally occurring Higgs boson [5]. Yet, so far, no sign of softly-broken weak scale SUSY has appeared at LHC [6, 7]. The growing mass gap between the weak scale– as typified by the W, Z and Higgs boson masses ~ 100 GeV– and the sparticle mass scale $m(\text{sparticle}) \gtrsim 1-2$ TeV has led to the re-emergence of the naturalness question: this time involving log rather than quadratic divergences.

Recent evaluations of supersymmetric models with radiatively-driven naturalness (RNS for radiatively-driven natural SUSY [8]) find that for a value of $\Delta_{\rm EW} < 10$ (30), then the gluino mass is bounded from above by $m_{\tilde{g}} \lesssim 2.5$ TeV (5 TeV). These $\Delta_{\rm EW}$ values correspond to $\Delta_{\rm EW}^{-1} = 10\%$ (3.3%) fine-tuning respectively. In contrast, the 5σ reach of LHC13 (LHC with $\sqrt{s} = 13$ TeV) for gluino pair production is estimated to be $m_{\tilde{g}} \sim 1.6$ TeV (100 fb^{-1}) and 1.9 TeV (1000 fb^{-1}) [9, 10]. In RNS models with gaugino mass unification, this reach can be extended via the same-sign diboson signature arising from wino pair production to equivalent values of $m_{\tilde{g}} \sim 2.4$ TeV for 1000 fb^{-1} [10, 11]. The upshot is that LHC13 may or may not have sufficient energy/luminosity to fully probe the entire parameter space of natural SUSY.[1]

Without a guaranteed path towards SUSY discovery, other alternatives have been explored. Many recent investigations promote Higgs boson profiling as a probe for physics beyond the SM. Since the Higgs boson h is now discovered, the goal is to measure every possible property of h to see if they maintain consistency with the SM or produce deviations which might point to new physics. These quantities include: the mass and width of the Higgs boson, its spin (which is essentially already determined to be spin-0 [14]) and its coupling strengths to various SM and non-SM decay modes. The coupling strengths κ_i are usually parametrized in terms of the SM values. Thus, $\kappa_b \equiv g_{hb\bar{b}}/g_{hb\bar{b}}(\text{SM})$, $\kappa_Z \equiv g_{hZZ}/g_{hZZ}(\text{SM})$, *etc.*. Evidence for beyond the SM (BSM) physics would then occur from the measurement of one or more κ_i values ($i = \tau, b, t, Z, W, g, \gamma$) to significantly differ (by several error bars) from the SM value of 1.

The capability of various accelerator options to measure the κ_i values has been analyzed [15, 16] and tabulated in Ref's. [17, 18]. In fact, early data from LHC8 seemed to indicate an enhancement in the Higgs to diphoton coupling which could have been construed as requiring new TeV-scale charged particles that circulate in the $h\gamma\gamma$ loop [19–21]. However, the current profile of the Higgs boson is consistent with SM predictions: *i.e.*, at present the Higgs boson appears to be "the" SM Higgs boson as no credible deviations from the SM have been found. As more data accrue from various collider options, the error bars on the various Higgs observables will tighten, and may reveal physics beyond the SM [22–24].

A particularly interesting scenario which merits investigation is that of natural supersym-

[1]Prospects for LHC13 indirect searches for RNS via initial state radiation off of higgsino pair production reactions (monojet signal) seem pessimistic [12]. Allowing for monojet radiation off of $\widetilde{Z}_1\widetilde{Z}_2$ production, $\widetilde{Z}_2 \to \widetilde{Z}_1\ell^+\ell^-$ may allow probes of the higgsino mass μ up to ~ 200 GeV assuming ~ 1000 fb^{-1} of integrated luminosity [13].

metry. In fact, several previous works have already investigated this case: Ref's. [25–29]. These papers all investigated models with light third generation squarks which are a consequence of minimizing the "large log" contribution to the Higgs boson mass: $\delta m_h^2 \sim -\frac{3f_t^2}{8\pi^2}(m_{Q_3}^2 + m_{U_3}^2 + A_t^2)\ln(\Lambda/m_{\rm SUSY})$, where f_t is the top Yukawa coupling, Λ is the cutoff scale, $m_{\rm SUSY}^2 = m_{\tilde{t}_1}m_{\tilde{t}_2}$ is the SUSY-breaking scale, and $m_{Q_3}^2$, $m_{U_3}^2$, and A_t denote the soft masses and the A-term for stops, respectively. The validity of this measure has been challenged in Ref's. [30,31] in that it sets to zero additional dependent contributions which lead to large cancellations. Alternatively, it is argued that the correct measure is $\Delta_{\rm EW}$ which instead requires 1. that the SUSY μ term is comparable to the weak scale ($m_{\rm weak} \sim 100$ GeV as typified by the W, Z and h masses), 2. that $m_{H_u}^2$ is driven radiatively to negative values of magnitude comparable to $m_{\rm weak}$ and 3. that radiative corrections to the weak scale effective potential[2] (which determines the electroweak vacuum expectation values (VEVs) and hence the Z-boson mass m_Z) are comparable or less than $m_{\rm weak}$. This latter condition is met for highly mixed but TeV-scale top-squarks, *i.e.*, much heavier than values expected from large log minimization. Meanwhile, the first of these conditions implies a spectrum of four higgsino-like states $\widetilde{Z}_{1,2}, \widetilde{W}_1^{\pm}$ with the $\widetilde{Z}_1$ as a higgsino-like lightest SUSY particle (LSP) and candidate for dark matter. If naturalness is required as well in the QCD sector, then the axion solution to the strong CP problem is invoked [32]. The SUSY DFSZ axion model [33] not only tames the strong CP problem but also provides an elegant solution to the SUSY μ problem. In this class of models, the apparent Little Hierarchy as typified by $\mu \ll m$(sparticle) can be naturally generated via a radiative breakdown of Peccei-Quinn symmetry [34,35].

While we agree with the assessment of Ref. [36] that unnatural SUSY is likely to be wrong SUSY, we would disagree with the assessment that the minimal supersymmetric Standard Model (MSSM) is at present fine-tuned over all of parameter space. While many SUSY models are indeed fine-tuned under $\Delta_{\rm EW}$ [31], the class of SUSY models with radiatively-driven naturalness (RNS) remain highly natural. The reason is that the current experimental limits on the SUSY μ parameter arise from negative searches for chargino pair production at LEP2: $m_{\widetilde{W}_1} > 103.5$ GeV. Roughly speaking then, μ is also $\gtrsim 100$ GeV. This value is quite close to the value of m_Z so that we can interpret the fact that m_W, m_Z and m_h are all clustered near 100 GeV as a consequence of μ^2, $m_{H_u}^2$(weak) and Σ_u^u all being comparable to– or lighter than-(100 GeV)^2. Meanwhile, the other soft SUSY breaking parameters can be much heavier, as is indicated by LHC sparticle search limits and radiative corrections to m_h.

As mentioned above, the class of RNS models predict light higgsino-like states around the electroweak scale. In addition, there may also be electroweak gauginos and/or heavy Higgs bosons below the TeV scale, which are currently less constrained as they are un-colored particles. The presence of such particles can in principle modify the Higgs couplings. For instance, the chargino loop contribution can alter the $h\gamma\gamma$ coupling $g_{h\gamma\gamma}$ if the chargino state has a sizable wino component. Also, if heavy Higgs bosons have relatively small masses, the lightest Higgs-boson couplings deviate from those in the case of decoupling limit, *i.e.*, the SM Higgs ones. The precise measurements of the Higgs couplings, therefore, may provide a way of probing the RNS scenario indirectly. Since forthcoming collider experiments can offer significantly improved sensitivities, it is quite important to investigate whether these experiments can actually observe

[2] Σ_u^u and Σ_d^d are given in the Appendix of Ref. [8].

any deviations in Higgs couplings in the case of RNS models.

In this paper, we calculate the deviations to the Higgs boson couplings $\kappa_{\tau,b,t,W,Z,g,\gamma}$ in supersymmetric models with low $\Delta_{\rm EW}$. After a brief review of our naturalness considerations in Sec. 2, in Sec. 3 we discuss the Higgs couplings in the MSSM and in Sec. 4 we discuss constraints on natural SUSY parameter space. We present in Sec. 5 our main results of the values of the κ_i versus electroweak naturalness measure $\Delta_{\rm EW}$ from a scan over parameters of the two-extra parameter non-universal Higgs (NUHM2) supergravity (SUGRA) model [37] which allows solutions with $\Delta_{\rm EW}$ as low as 5–10. We compare these expectations against the values which are expected to be probed at present and future LHC runs, and with expectations from the International Linear e^+e^- Collider (ILC). In SUSY models with low $\Delta_{\rm EW}$ (highly natural models), the bulk of points give tiny deviations from SM expectation. In Sec. 6, we show that the value of κ_γ can be enhanced to yield deviations as high as only 2% in models with gaugino mass non-universality and a light wino [38]. In Sec. 7, we compare our results against direct sparticle search prospects for LHC and ILC. We stress there that LHC13 has only a limited reach for natural SUSY. In addition, if the ILC is built initially as a Higgs factory, we ultimately expect from natural SUSY that the Higgs profile will look very SM-like: any major deviation from the SM κ_i would likely come from a rather light spectrum of heavy Higgs bosons which are already highly constrained by LHC searches. We find that the best prospect for probing natural supersymmetric models remains as the direct production of higgsino pairs at ILC. In such a case, ILC would function as a higgsino factory and as a discovery machine for SUSY [39].

2 A natural SUSY spectrum

Any quantitative discussion of naturalness requires the use of some measure, and several have appeared in the literature. Before proceeding, however, we note the observation that some measures can be mis-applied by claiming large opposite-sign contributions to observables of *dependent* quantities: these mis-applications lead to over-estimates [30] of electroweak fine-tuning.[3]

To avoid such pitfalls, any naturalness measure should obey the fine-tuning rule [31]: *When evaluating fine-tuning, it is not permissible to claim fine-tuning of* **dependent** *quantities one against another.*

2.1 Electroweak scale naturalness

The relationship between the weak scale $m_{\rm weak}$ and SUSY parameters arises from minimizing the MSSM scalar potential. One is led to the relation [40]

$$\frac{m_Z^2}{2} = \frac{m_{H_d}^2 + \Sigma_d^d - (m_{H_u}^2 + \Sigma_u^u)\tan^2\beta}{\tan^2\beta - 1} - \mu^2 \ , \tag{1}$$

for the Z mass m_Z, where Σ_u^u and Σ_d^d denote the 1-loop corrections (expressions can be found in the Appendix of Ref. [8]) to the scalar potential, $m_{H_u}^2$ and $m_{H_d}^2$ are the Higgs soft masses, and

[3]For example, if an observable $\mathcal{O}$ is expressed as $\mathcal{O} = \mathcal{O} + b - b$ where b is large, then $\mathcal{O}$ may look fine-tuned. In this trivial example, combining dependent contributions then cancels the would-be source of fine-tuning.

$\tan\beta \equiv \langle H_u\rangle/\langle H_d\rangle$ is the ratio of the Higgs VEVs. SUSY models requiring large cancellations between the various terms on the right-hand-side of Eq. (1) to reproduce the measured value of m_Z^2 are regarded as unnatural, or fine-tuned. In contrast, SUSY models which generate terms on the RHS of Eq. (1) which are all less than or comparable to $m_{\rm weak}$ are regarded as natural. Thus, the *electroweak* naturalness measure $\Delta_{\rm EW}$ is defined as [8, 41]

$$\Delta_{\rm EW} \equiv \max|\text{each additive term on RHS of Eq. (1)}|. \tag{2}$$

Including the various radiative corrections, over 40 terms contribute. Neglecting radiative corrections, and taking moderate-to-large $\tan\beta \gtrsim 3$, then $m_Z^2/2 \sim -m_{H_u}^2 - \mu^2$ so the main criterion for naturalness is that at the weak scale $m_{H_u}^2 \sim -m_Z^2$ and $\mu^2 \sim m_Z^2$ [42]. The value of $m_{H_d}^2$ (where $m_A \sim m_{H_d}$(weak) with m_A being the mass of the CP-odd Higgs boson) can lie in the TeV range since it is suppressed by $1/\tan^2\beta$. The largest radiative corrections come from the top squark sector. Requiring highly mixed TeV-scale top squarks minimizes $\Sigma_u^u(\tilde{t}_{1,2})$ whilst lifting the Higgs mass m_h to ~ 125 GeV [8].

Some virtues of $\Delta_{\rm EW}$ include 1. that it is model independent so that any model generating the same weak scale spectrum will have the same naturalness value and 2. it obeys the fine-tuning rule. It is also predictive: since $|\mu| \sim m_Z$, it implies a spectrum of four higgsino states $\widetilde{Z}_{1,2}$ and $\widetilde{W}_1^{\pm}$ all lying not-too-far from m_Z: $\mu \sim 100-200$ GeV. While many models are indeed highly fine-tuned under $\Delta_{\rm EW}$ [31, 43], the NUHM2 model and its generalizations admit $\Delta_{\rm EW}$ values as low as $5-10$ leading to just $10-20\%$ electroweak fine-tuning. The models with low $\Delta_{\rm EW} \lesssim 30$ are regarded as *natural*.

2.2 Higgs mass fine-tuning

An alternative measure comes from Higgs mass fine-tuning [44–46]. The light Higgs mass for $\tan\beta \gtrsim 3$ is given by

$$m_h^2 \sim -2\{m_{H_u}^2(\Lambda) + \delta m_{H_u}^2 + \mu^2\}\ , \tag{3}$$

where the largest contribution to $\delta m_{H_u}^2$ includes divergent logarithms of the effective theory cut-off scale Λ which is commonly taken to be $\Lambda \simeq m_{\rm GUT} \sim 2\times 10^{16}$ GeV in gravity-mediation. By neglecting gauge terms and setting $m_{H_u}^2$ to zero, a one step integration of the renormalization group equation (RGE) for $m_{H_u}^2$ leads to $\delta m_{H_u}^2 \sim -\frac{3f_t^2}{8\pi^2}(m_{Q_3}^2+m_{U_3}^2+A_t^2)\ln(\Lambda/m_{\rm SUSY})$. Requiring $\delta m_{H_u}^2 \lesssim m_h^2$ then implies the existence of three third generation squarks $\tilde{t}_{1,2}$, $\tilde{b}_1$ with mass less than about 600 GeV [46]. It also leads to claims that SUSY is fine-tuned at the per-mille level [47].

The problem with this measure is that $m_{H_u}^2$ and $\delta m_{H_u}^2$ are not independent.[4] In fact, the larger the value of $m_{H_u}^2(\Lambda)$ becomes, then the larger becomes the cancelling correction [48]. By combining the dependent terms $(m_{H_u}^2(\Lambda) + \delta m_{H_u}^2)$, then instead one is lead to requiring that μ^2 and the *weak scale value* of $m_{H_u}^2$ are both comparable to m_h^2. Even if $m_{H_u}^2(\Lambda)$ lies in the multi-TeV range, it can be driven to small negative squared values at the weak scale $m_{\rm weak}$ via the same radiative corrections that drive electroweak symmetry breaking in SUGRA models.

[4]This is different from the case of the SM Higgs mass fine-tuning where the tree level mass and quadratic divergences are independent.

After combining dependent contributions to m_h^2, then a low Higgs mass fine-tuning implies the same general consequences as those of low $\Delta_{\rm EW}$.

2.3 BG fine-tuning

The BG measure [49–51] is defined as

$$\Delta_{\rm BG} = {\rm max}_i \left| \frac{\partial \log m_Z^2}{\partial \log p_i} \right| \ , \tag{4}$$

where p_i are fundamental (usually high scale) parameters of the model labeled by index i. To evaluate, we start with the weak scale relation

$$m_Z^2 \simeq -2\mu^2({\rm weak}) - 2m_{H_u}^2({\rm weak}) \ , \tag{5}$$

and express the right-hand-side in terms of fundamental high scale parameters. A pitfall can occur in what constitutes high scale independent parameters. Since μ hardly evolves during the renormalization group (RG) flow– it only receives the wave-function renormalization thanks to the non-renormalization theorem of the superpotential– then $\mu({\rm weak}) \sim \mu(\Lambda)$. On the other hand, $m_{H_u}^2$ evolves greatly: indeed, it must be driven through zero to negative values by the large top quark Yukawa coupling f_t for electroweak symmetry to be broken radiatively. Semi-analytic solutions to the $m_{H_u}^2$ RGE allows $m_{H_u}^2({\rm weak})$ to be evaluated as a large sum of contributions from various high scale soft parameters: some positive and some negative. In the case of gravity-mediation, however, for any particular hidden sector the high-scale soft terms are all calculable as multiples of the gravitino mass $m_{3/2}$ [52]. If we vary $m_{3/2}$, the soft terms all vary accordingly: *i.e.* they are *not independent* in SUGRA models. By combining the dependent soft SUSY breaking terms, then the Z mass can be expressed as [31]

$$m_Z^2 \simeq -2\mu^2(\Lambda) - am_{3/2}^2 \ , \tag{6}$$

with a being a certain proportionality factor dependent on each soft mass spectrum. Using Eq. (6)– and since μ hardly evolves from Λ to $m_{\rm weak}$– we have $am_{3/2}^2 \simeq 2m_{H_u}^2({\rm weak})$. Even if $m_{3/2}$ is large (as implied by LHC8 limits for gravity-mediation), then one may still generate natural models if the coefficient a is small. Under the combination of dependent soft SUSY breaking terms, then low $\Delta_{\rm BG}$ implies the same as low $\Delta_{\rm EW}$: that $\mu \sim m_{\rm weak}$ and that $m_{H_u}^2$ is driven to small and not large negative values.

3 Higgs couplings in the MSSM

In this Section, we briefly review the Higgs couplings to SM particles. In the MSSM, the lighter of the two CP-even Higgs mass eigenstates is typically a SM-like Higgs boson but with properties differing from the SM case depending on the mixing angle α. In general, the Higgs boson couplings to vector bosons (W and Z bosons) are simply determined by α and β while couplings to fermions have contributions from loop corrections as well. On the other hand, the dimension-five couplings of Higgs to diphoton and to digluon are generated at one-loop order.

Note that also in the SM these couplings are induced at loop level. For this reason, these couplings can be rather sensitive to the SUSY effects.

In the MSSM, the SM-like Higgs boson is usually the lighter eigenstate of the mass matrix

$$\mathcal{M}_h^2 = \begin{pmatrix} m_{H_u}^2 + \mu^2 + m_Z^2(1-2\cos 2\beta)/2 & -(m_{H_u}^2 + m_{H_d}^2 + 2\mu^2 + m_Z^2)\sin 2\beta/2 \\ -(m_{H_u}^2 + m_{H_d}^2 + 2\mu^2 + m_Z^2)\sin 2\beta/2 & m_{H_d}^2 + \mu^2 + m_Z^2(1+2\cos 2\beta)/2 \end{pmatrix} + \delta\mathcal{M}_h^2 \tag{7}$$

in the basis of the weak eigenstates of the CP-even neutral Higgs fields (h_{uR}^0, h_{dR}^0). The radiative corrections to the Higgs mass-squared matrix are included in $\delta\mathcal{M}_h^2$. It is worth noting that we use Higgs soft masses and μ in order to directly compare it with fine-tuning argument in Eq. (3). The conventional form of mass matrix is obtained if one uses the relations,

$$\begin{aligned} m_A^2 &= m_{H_u}^2 + m_{H_d}^2 + 2\mu^2 \\ &= \frac{1}{\cos^2\beta}\left(m_{H_u}^2 + \mu^2 - \frac{1}{2}m_Z^2\cos 2\beta\right) \\ &= \frac{1}{\sin^2\beta}\left(m_{H_d}^2 + \mu^2 + \frac{1}{2}m_Z^2\cos 2\beta\right), \end{aligned} \tag{8}$$

from the electroweak symmetry breaking conditions. The mass-squared matrix $\mathcal{M}_h^2$ is diagonalized by the mixing matrix[5]

$$\begin{pmatrix} h \\ H \end{pmatrix} = \begin{pmatrix} \cos\alpha & \sin\alpha \\ -\sin\alpha & \cos\alpha \end{pmatrix} \begin{pmatrix} h_{uR}^0 \\ h_{dR}^0 \end{pmatrix} . \tag{9}$$

The vector boson couplings are simply given by

$$g_{hVV} = g_{hVV}^{\rm SM}\sin(\alpha+\beta) \quad \text{for} \quad V = W, Z. \tag{10}$$

In the decoupling limit where $m_A \gg m_Z$, the mixing angle α follows the relation, $\alpha+\beta \simeq \pi/2$. This decoupling behavior can be clearly seen in the approximate formula [53]:

$$\cos(\alpha+\beta) = \frac{m_Z^2\sin 4\beta}{2m_A^2}\left(1 - \frac{\delta\mathcal{M}_{h,11}^2 - \delta\mathcal{M}_{h,22}^2}{2m_Z^2\cos 2\beta} - \frac{\delta\mathcal{M}_{h,12}^2}{m_Z^2\sin 2\beta}\right) + \mathcal{O}\left(\frac{m_Z^4}{m_A^4}\right). \tag{11}$$

Note that if the radiative corrections in Eq. (11) are sub-dominant, then $\cos(\alpha+\beta) < 0$ since $\sin 4\beta < 0$. This determines the direction of the deviation in the Higgs-fermion couplings, as we will discuss below. The above equation reads

$$\sin(\alpha+\beta) \simeq 1 - \frac{1}{2}\cos^2(\alpha+\beta) = 1 - \mathcal{O}\left(\frac{m_Z^4}{m_A^4}\right). \tag{12}$$

From this relation, one can easily see that $\cos(\alpha+\beta) \to 0$ and $\sin(\alpha+\beta) \to 1$ as $m_A \to \infty$.[6] In addition, we note that the deviations in the gauge boson couplings from the SM ones rapidly

[5] In the notation of Ref. [40], the Higgs mixing angle α is the negative of other conventions.

[6] It is also the case that $\cos(\alpha+\beta) \to 0$ for fixed m_A when $\tan\beta \to 1$ ($\beta \to 45^\circ$). In this situation, the value of m_h drops below its measured range so we neglect this case.

decrease in the large m_A limit since they are suppressed by a factor of m_Z^4/m_A^4. Thus, we expect that the vector boson couplings are almost SM-like, as will be actually seen in Sec. 5.

For the case of fermion couplings, we need to consider an effective Lagrangian[7] for the Yukawa couplings. Including SUSY threshold loop-corrections, the low-energy effective Yukawa terms below the SUSY breaking scale are written as [55, 56]

$$-\mathcal{L}_{\rm eff} = (f_b + \delta f_b)\bar{b}_R H_d Q_3 + \Delta f_b \bar{b}_R H_u^* Q_3 + (f_t + \delta f_t)\bar{t}_R H_u Q_3 + \Delta f_t \bar{t}_R H_d^* Q_3 + \text{h.c.}, \tag{13}$$

where δf_b and δf_t represent the radiative corrections to the tree-level bottom and top Yukawa couplings f_b and f_t in the MSSM superpotential, respectively, while Δf_b and Δf_t are loop-induced non-holomorphic Yukawa couplings. Notice that these (non-logarithmic) radiative corrections are generated by the SUSY breaking effects; in the SUSY limit, the vertex corrections to the Yukawa couplings vanish because of the non-renormalization theorem. These radiative corrections modify the relations between the fermion masses and the corresponding Yukawa couplings as

$$m_b = f_b v \cos\beta \left(1 + \frac{\delta f_b}{f_b} + \frac{\Delta f_b}{f_b}\tan\beta\right) \equiv f_b v \cos\beta (1 + \Delta_b) \ , \tag{14}$$

$$m_t = f_t v \sin\beta \left(1 + \frac{\delta f_t}{f_t} + \frac{\Delta f_t}{f_t}\cot\beta\right) \equiv f_t v \sin\beta (1 + \Delta_t) \ , \tag{15}$$

where $v \simeq 174$ GeV denotes the Higgs VEV and $\Delta_{b,t}$ are given by

$$\Delta_b \simeq \left[\frac{2\alpha_s}{3\pi} M_3 \mu I(m_{\tilde{b}_1}^2, m_{\tilde{b}_2}^2, M_3^2) + \frac{f_t^2}{16\pi^2}\mu A_t I(m_{\tilde{t}_1}^2, m_{\tilde{t}_2}^2, \mu^2)\right]\tan\beta \ , \tag{16}$$

$$\Delta_t \simeq -\left[\frac{2\alpha_s}{3\pi} M_3 A_t I(m_{\tilde{t}_1}^2, m_{\tilde{t}_2}^2, M_3^2) + \frac{f_b^2}{16\pi^2}\mu^2 I(m_{\tilde{b}_1}^2, m_{\tilde{b}_2}^2, \mu^2)\right] \ . \tag{17}$$

Here, α_s denotes the strong gauge coupling constant. M_3 and $m_{\tilde{b}_{1,2}}$ are the masses of gluino and sbottoms, respectively. The loop function is defined by

$$I(a,b,c) = \frac{ab\ln(a/b) + bc\ln(b/c) + ca\ln(c/a)}{(a-b)(b-c)(a-c)} \ . \tag{18}$$

This function is of the order of $1/\max\{a^2, b^2, c^2\}$ [55]. Notice that for large $\tan\beta$, $\Delta_b \simeq \Delta f_b \tan\beta / f_b$ since the non-holomorphic correction is enhanced by $\tan\beta$. The non-holomorphic correction to the top Yukawa coupling is, on the other hand, suppressed by $\tan\beta$, and thus $\Delta_t \simeq \delta f_t / f_t$ in this case. The modifications in the relations (14) and (15), as well as the deviation from the decoupling limit characterized by Eq. (11), change the fermion-Higgs couplings from

[7] In our analysis, the low-energy effective theory is matched onto the full MSSM at the scale of $m_{\rm SUSY} \equiv (m_{\tilde{t}_1} m_{\tilde{t}_2})^{\frac{1}{2}}$ in the $\overline{\rm DR}$-scheme [54], with $m_{\tilde{t}_{1,2}}$ being the masses of stops.

the SM ones. We have[8]

$$g_{hbb} = g_{hbb}^{\rm SM}\left[\sin(\alpha+\beta) - \frac{\cos(\alpha+\beta)}{1+\Delta_b}\left\{\tan\beta - \Delta_b\cot\beta + (\tan\beta+\cot\beta)\frac{\delta f_b}{f_b}\right\}\right] , \quad (21)$$

$$g_{htt} = g_{htt}^{\rm SM}\left[\sin(\alpha+\beta) + \frac{\cos(\alpha+\beta)}{1+\Delta_t}\left\{(1+\Delta_t)\cot\beta - (1+\cot^2\beta)\frac{\Delta f_t}{f_t}\right\}\right] . \quad (22)$$

Here we express the latter equation in terms of Δ_t and Δf_t since $\Delta_t \simeq \delta f_t/f_t$. One can also obtain a similar relation for the Higgs coupling to tau lepton, $g_{h\tau\tau}$, by replacing Δ_b with Δ_τ and $\delta f_b/f_b$ with $\delta f_\tau/f_\tau$ in Eq. (21). In this case Δ_τ is dominantly induced by the wino-higgsino loop diagram [57]:

$$\Delta_\tau \simeq -\frac{3\alpha_2}{8\pi} M_2\mu\tan\beta I(m^2_{\tilde{\tau}_L}, M_2^2, \mu^2) , \quad (23)$$

where α_2 is the $\mathrm{SU}(2)_L$ gauge coupling constant, M_2 is the wino mass, and $m_{\tilde{\tau}_L}$ is the left-handed third generation slepton mass. Here, we have dropped the sub-dominant bino contribution for brevity. From the above equations, it is found that the deviation from the SM couplings is proportional to m_Z^2/m_A^2 and therefore becomes quite small in the large m_A limit. In addition, we see that the deviation in the bottom and tau couplings is enhanced by $\tan\beta$, while that in the top coupling is not. Thus, the bottom and tau couplings are more appropriate to probe the SUSY effects than the top coupling, as will be shown below. Moreover, we note that as long as the radiative corrections are moderate, the bottom/tau (top) coupling is always larger (smaller) than the SM one as $\cos(\alpha+\beta) < 0$. This feature is also found in the analysis given in Sec. 5.

For the various Higgs couplings to gg pairs, we use the standard expressions including quark and squark triangle diagrams as given in Ref's [58]. We find that the SUSY effect on the effective gluon coupling is dominantly given by the stop contribution, which can be approximately expressed as [59]

$$\kappa_g \simeq 1 + \frac{m_t^2}{4}\left[\frac{1}{m^2_{\tilde{t}_1}} + \frac{1}{m^2_{\tilde{t}_2}} - \frac{(A_t - \mu\cot\beta)^2}{m^2_{\tilde{t}_1} m^2_{\tilde{t}_2}}\right] . \quad (24)$$

This expression shows that $\kappa_g < 1$ occurs only if the stop mixing is sizable. As discussed above, the RNS scenario with $m_h \simeq 125$ GeV requires large stop mixing, and thus we expect that the gluon coupling can be smaller than the SM one in this scenario.

For the Higgs couplings to $\gamma\gamma$, we use standard expressions including quark, lepton, squark, slepton, $W^\pm$, $H^\pm$ and $\widetilde{W}^\pm_{1,2}$ loops [58]. In the RNS models, higgsinos lie around the electroweak scale, and thus may give rise to a considerable contribution to the $\gamma\gamma$ coupling if the higgsinos well mix with winos to have a sizable coupling with the Higgs boson. This can be achieved when wino has a relatively small mass. We discuss this possibility in Sec. 6.

[8]Here, we have used the identities

$$\frac{\sin\alpha}{\cos\beta} = \sin(\alpha+\beta) - \tan\beta\cos(\alpha+\beta), \quad (19)$$

$$\frac{\cos\alpha}{\sin\beta} = \sin(\alpha+\beta) + \cot\beta\cos(\alpha+\beta). \quad (20)$$

4 Constraints from B and Higgs decays

We next discuss some low energy observables that constrain the low m_A region in our scanned results as shown in the next Section. As discussed in the previous Section, Higgs couplings to vector bosons and fermions suffer deviations mainly from Higgs mixing so that large deviations in the κ_i are mainly expected when m_A is small. In such cases, however, loop-mediated contributions to B decays and also tree-level contribution mediated by charged Higgs also become larger. In this case, B-decay observables can constrain this portion of parameter space. In addition, there exist tight constraints on low $m_{A,H}$ in the m_A vs. $\tan\beta$ plane from Atlas/CMS searches for s-channel $gg \to A, H$ production followed by $A, H \to \tau^+\tau^-$.

4.1 $BF(B \to X_s\gamma)$

For our evaluation, we use the NLO SUSY calculation from Ref. [60] as included in Isatools. In the MSSM, the two major SUSY contributions come from chargino-stop loops and also from the charged Higgs-top loop. In the large $\tan\beta$ regime, these are approximately given by

$$BF(B \to X_s\gamma)|_{\widetilde{W},\tilde{t}} \;\propto\; \mu A_t \tan\beta \frac{m_b}{v(1+\Delta_b)} f(m_{\tilde{t}_1}, m_{\tilde{t}_2}, m_{\widetilde{W}}), \tag{25}$$

$$BF(B \to X_s\gamma)|_{H^\pm,t} \;\propto\; \frac{m_b(f_t\cos\beta - \Delta f_t \sin\beta)}{v\cos\beta(1+\Delta_b)} g(m_{H^\pm}, m_t) \tag{26}$$

where f and g are loop functions [61]. In order to lift the Higgs mass to 125 GeV, it is normally required that stop masses are of order TeV although one of them can be below TeV if the maximally-mixed stop scenario is considered. In such a case, then the chargino-stop loop contributions are usually small. For the small m_A case– where Higgs mixing can sizably affect vector boson and fermion couplings– the light charged Higgs ($m^2_{H_\pm} \simeq m^2_A + m^2_W$) can make a sizable contribution to the decay width. In this case, the small m_A region is typically excluded by the $BF(B \to X_s\gamma)$ measurement.

4.2 $BF(B_s \to \mu^+\mu^-)$

The $B_s \to \mu^+\mu^-$ decay is induced by flavor changing interactions of Higgs bosons, h, H, and A. The flavor changing couplings of Higgs with b- and s-quarks are generated by similar loop processes as those for Δ_b and Δ_t. The physical discussion and calculation details are provided in Ref. [62]. Since $g_{hbs} \propto \cos(\alpha+\beta)/\cos^2\beta$, $g_{Hbs} \propto -\sin(\alpha+\beta)/\cos^2\beta$ and $g_{Abs} \propto -1/\cos^2\beta$, the dominant contributions are from H and A mediated processes. The overall branching fraction is then given by

$$BF(B_s \to \mu^+\mu^-) \propto \tan^6\beta \frac{m_t^4}{m_A^4}. \tag{27}$$

Hence small m_A and large $\tan\beta$ enhance $BF(B_s \to \mu^+\mu^-)$, and thus the experimental bounds stringently restrict such a parameter region.

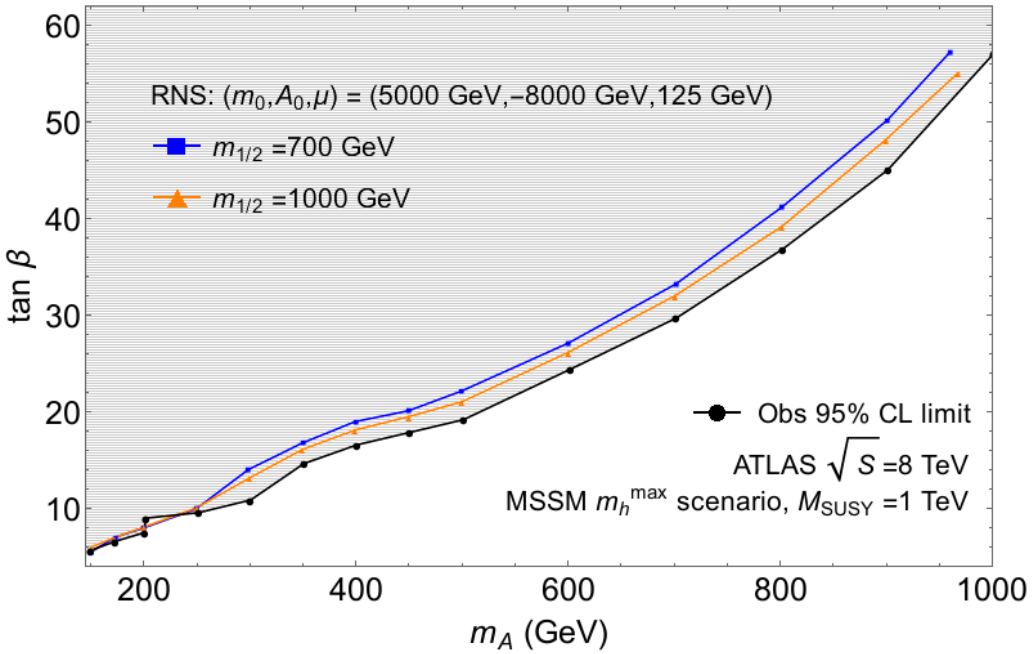

Figure 1: Plot of the Atlas bounds [63] on $gg \to A,\ H \to \tau^+\tau^-$ in the m_A vs. $\tan\beta$ plane in the m_h(max) scenario with $m_{\rm SUSY} = 1$ TeV. We re-cast these results as constraints in the RNS model with $m_0 = 5$ TeV, $A_0 = -8$ TeV, $\mu = 125$ GeV and with $m_{1/2} = 0.7$ and 1 TeV.

4.3 LHC8 constraints on $A,\ H \to \tau^+\tau^-$

The Atlas [63] and CMS [64] collaborations have searched for s-channel $gg \to A,\ H$ production followed by $A,\ H \to \tau^+\tau^-$ decays. These searches place strong constraints on SUSY Higgs models in the m_A vs. $\tan\beta$ plane. In evaluating these constraints, Atlas and CMS usually assume a heavy SUSY particle mass spectrum so that the $A,\ H$ decay entirely into SM modes. However, in the RNS model where $\mu \sim 100 - 200$ GeV, then SUSY decay modes into higgsino pairs should be open when $m_{A,H} \gtrsim 2\mu$. Since the heavy Higgs states couple to neutralinos via a product of gaugino times higgsino components [40], then the decay to higgsino pairs is somewhat suppressed. However, the decay to gaugino plus higgsino can dominate the heavy Higgs branching fractions if these decay modes are open: see Ref. [65] for explicit plots.

Given this situation, it is useful to re-cast the Atlas/CMS bounds for the case of RNS. We have performed this calculation with results shown in Fig. 1. Here, the production cross section [66] is proportional to $\Gamma(H, A \to gg)$ while the branching fractions $BF(A, H \to \tau^+\tau^-)$ are extracted from Isajet. Thus, we calculate $\Gamma(H, A \to gg) \times BF(A, H \to \tau^+\tau^-)$ for the $m_{\rm SUSY} = 1$ TeV case along the Atlas contour, and then equate this to the value calculated in the RNS model. In the RNS case, since the $BF(A, H \to \tau^+\tau^-)$ is diminished due to the presence of supersymmetric decay modes, one must compensate by increasing $\tan\beta$, which increases $\Gamma(A, H \to gg)$ via the b-quark loop.

The results from Fig. 1 show that for a given value of m_A, the excluded range of $\tan\beta$ just moves up just a few units. This is because for most of the range shown with $m_A < 1$ TeV the

potentially dominant A, H decay to wino+higgsino has not fully opened up: these decays tend to dominate the heavy Higgs branching fractions for $m_{A,H}$ in the multi-TeV region. In practise, to be conservative and since we do not wish to re-compute the Atlas bound for every different set of $m_{1/2}$ and μ values which are sampled, we will simply impose the Atlas constraint on all subsequent plots.

5 Results for RNS in NUHM2

In this Section, we explore the κ_i values which are expected in SUGRA GUT models with low fine-tuning $\Delta_{\rm EW}$. We will adopt the two-extra parameter non-universal Higgs model [37] (NUHM2) as a template. The parameters in this model are given by

$$m_0,\ m_{1/2},\ A_0,\ \tan\beta,\ \mu,\ m_A. \tag{28}$$

In the above set, m_0 is the GUT scale value of the common soft mass parameter for matter scalars, $m_{1/2}$ is the unified gaugino mass, A_0 is the unified trilinear soft term, $\tan\beta$ is the usual ratio of VEVs and μ and m_A are the weak scale values of the superpotential μ parameter and the pseudoscalar Higgs mass. These latter two determine the weak scale values of $m^2_{H_u}$ and $m^2_{H_d}$ from the scalar potential minimization conditions. The GUT scale values of $m^2_{H_u}$ and $m^2_{H_d}$ are determined by RG evolution and are then in general non-universal with the matter scalar mass m_0.

We generate a random scan over the parameter space

$$\begin{aligned} m_0 &: 0-20 \text{ TeV}, \\ m_{1/2} &: 0.5-2 \text{ TeV}, \\ -3 &< A_0/m_0 < 3, \\ \mu &: 0.1-1.5 \text{ TeV}, \\ m_A &: 0.15-20 \text{ TeV}, \\ \tan\beta &: 3-60, \end{aligned} \tag{29}$$

and generate sparticle mass spectra using Isajet 7.84 [67] which contains the Isasugra subprogram. The range of μ covers only positive values; the physical results are very similar in the case $\mu < 0$ except that $\Delta{\rm Br}(b\to s\gamma)$ limits are more constraining for low m_A and hence we get smaller deviations in the κ_i values. The major difference with negative μ is κ_γ which will be discussed in Sec. 6.

We require of our solutions that:

- electroweak symmetry be radiatively broken (REWSB),
- the neutralino $\widetilde{Z}_1$ is the lightest MSSM particle,
- the light chargino mass obeys the model independent LEP2 limit, $m_{\widetilde{W}_1} > 103.5$ GeV [68],
- LHC search bounds on $m_{\tilde{g}}$ and $m_{\tilde{q}}$ in mSUGRA are respected [6, 7],

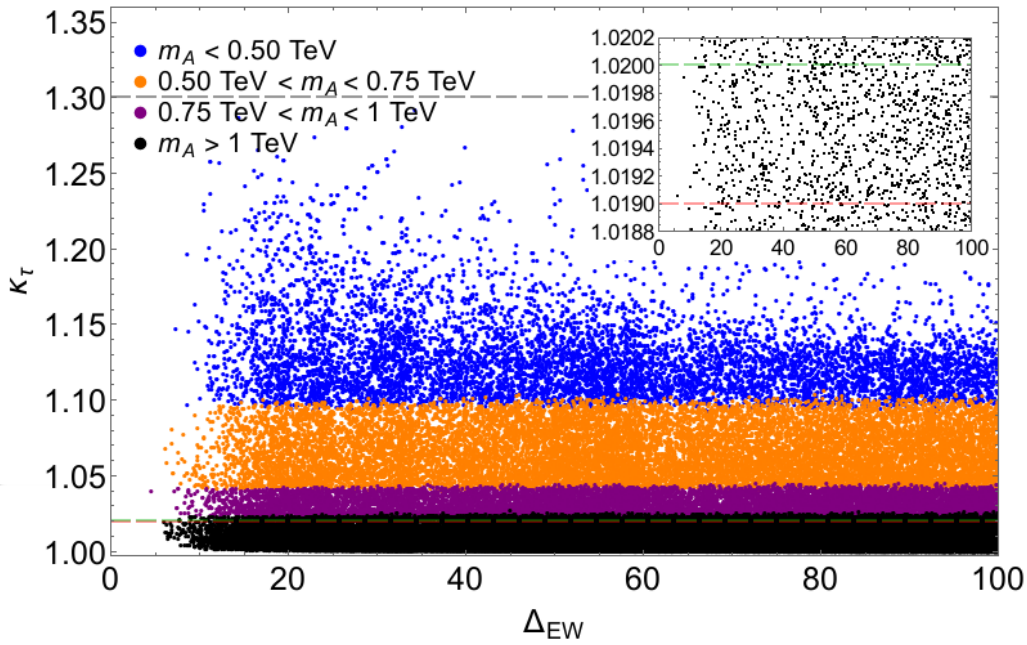

Figure 2: κ_τ vs. $\Delta_{\rm EW}$ from scan over NUHM2 parameter space with $m_h = 125 \pm 2$ GeV and LHC Higgs and sparticle mass constraints. The current LHC reach (gray-dashed) and future reach of LHC (green-dashed) and ILC (red-dashed) are shown (see the text for details).

- $-2.3 \times 10^{-9} < \Delta{\rm Br}(B_s \to \mu^+\mu^-) < 0.6 \times 10^{-9}$ [23]
- $-3.6 \times 10^{-5} < \Delta{\rm Br}(b \to s\gamma) < 9.2 \times 10^{-5}$ [23]
- LHC8 constraints on $A, H \to \tau^+\tau^-$ in the m_A vs. $\tan\beta$ plane are satisfied,
- $m_h = 125 \pm 2$ GeV.

Here, we have taken a ± 2 GeV error range in the Higgs mass m_h to reflect the theoretical uncertainty of the computation.[9] The lower bound on the Higgs mass rules out the region where $m_0 \lesssim 0.4$ TeV. The upper bound on the branching fraction of $b \to s\gamma$ decay removes the bulk of parameter region where $m_A \lesssim 0.3$ TeV.

Our first results are shown as κ_τ vs. $\Delta_{\rm EW}$ in Fig. 2. Here, the dots are color coded as to the value of m_A, with blue indicating $m_A < 0.5$ TeV, orange is 0.5 TeV $< m_A <$ 0.75 TeV, purple is 0.75 TeV $< m_A <$ 1 TeV and black is $m_A > 1$ TeV.[10] As discussed in Sec. 3, this coupling has a large deviation from unity if $\cos(\alpha + \beta)$ is sizable, which occurs when m_A is comparable to m_h. Thus, the magnitude of κ_τ follows the mass values for the heavy Higgs eigenstates: a value of $\kappa_\tau \sim 1$ when the heavy Higgs eigenstates decouple. Furthermore, in a wide range of parameter space κ_τ is larger than unity, as discussed in Sec. 3. In the RNS model with

[9] We implement the RG-improved 1-loop effective potential calculation of m_h which includes leading 2-loop terms in Isajet.

[10] We have also plotted with color-coding according to $m_A/\tan\beta$ values. We did not glean any additional insight from these plots.

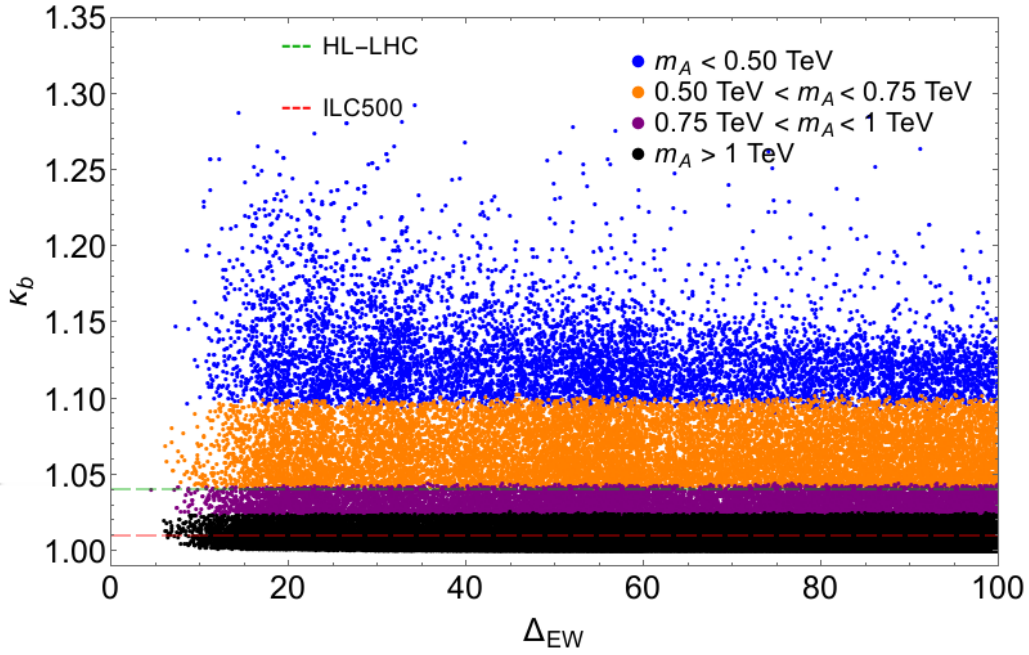

Figure 3: κ_b vs. $\Delta_{\rm EW}$ from scan over NUHM2 parameter space with $m_h = 125 \pm 2$ GeV and LHC Higgs and sparticle mass constraints.

low $\Delta_{\rm EW}$, $|\mu| \sim m_Z$ and $|m_{H_d}| \sim m_A$. Since $m^2_{H_d}$ enters $\Delta_{\rm EW}$ as $\sim m^2_{H_d}/\tan^2\beta$, then rather large values of m_A are consistent with low fine-tuning. Upper limits on m_A have been found in Ref. [65] where $m_A < 5-8$ TeV for $\Delta_{\rm EW} < 30$ (the exact upper bound depends on $\tan\beta$). Thus, the bulk of points with relatively large m_A and low $\Delta_{\rm EW}$ are expected to give only slight deviations from the SM $h\tau\tau$ coupling. The points with large deviations occur for low m_A, and in fact many of these points are subject to the previously mentioned constraints from LHC on $gg \to h, H, A \to \tau^+\tau^-$ for SUSY in the m_A vs. $\tan\beta$ plane [63]. Points in violation of the LHC $H, A \to \tau^+\tau^-$ constraint have been excluded from our plots.

In the plot, we also show the current reach for κ_τ from LHC8 as the gray dashed line at $\kappa_\tau \sim 1.3$ and the future reach of high luminosity LHC13 (HL-LHC) with 3000 fb^{-1} and ILC500 in the green- and red-dashed lines, respectively [17, 18]. From current reach of LHC8, we can conclude that the LHC experiment has already disfavored mass spectra with $m_A < 300$ GeV. Furthermore, it turns out that the high-luminosity LHC as well as the ILC can probe $m_A \sim 1$ TeV, which can be clearly seen in the inset of the figure where a magnified view of κ_τ very close to 1 is shown. While future colliders can probe much of the parameter space with low $\Delta_{\rm EW}$, a large chunk with multi-TeV values of m_A would look very SM-like.

In Fig. 3, we show κ_b vs. $\Delta_{\rm EW}$. The locale of the dots is nearly the same as for the κ_τ plot since $\kappa_b \simeq \kappa_\tau$. The main difference occurs in the current and future collider reach for κ_b. Here, HL-LHC is expected to probe a 4% deviation while ILC500 can probe a 1% deviation. While these reach values probe a large fraction of parameter space with $m_A \lesssim 1$ TeV, there are a number of natural models which predict quite small deviation in κ_b.

In Fig. 4, we show the values of κ_t vs. $\Delta_{\rm EW}$. As discussed in Sec. 3, this coupling is expected

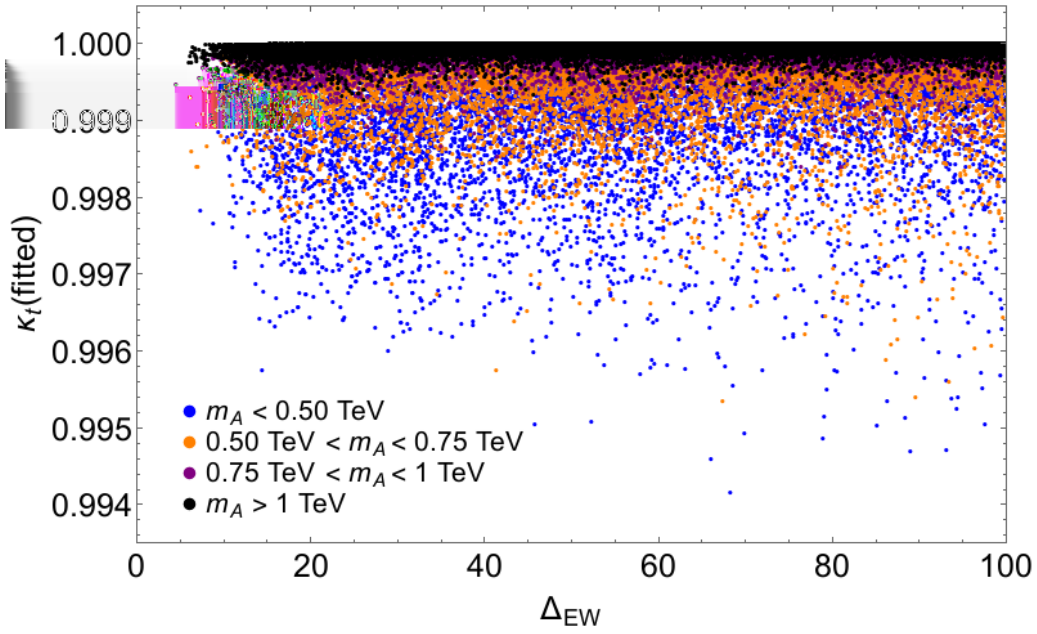

Figure 4: κ_t vs. $\Delta_{\rm EW}$ from scan over NUHM2 parameter space with $m_h = 125 \pm 2$ GeV and LHC Higgs and sparticle mass constraints.

to suffer hardly any deviation from the SM value, since there is no $\tan\beta$ enhanced effect in this case. In addition, the projected experimental probes are much more limited since the $h \to t\bar{t}$ decay mode is kinematically closed. The value of κ_t must be extracted from fits to the Higgs production coupling hgg which includes a top-quark loop in the case of LHC, and also to $t\bar{t}h$ production in the case of LHC and ILC. Here, it is expected that ILC500 may probe to the 2.5% level ($\kappa_t \sim 0.975$) once $\sqrt{s} > 2m_t + m_h$.

In Fig. 5, we show the values of κ_Z vs. $\Delta_{\rm EW}$. In this case, the value of $\kappa_{W,Z}$ is expected to be close to 1 since the deviation is suppressed by m_Z^4/m_A^4 as shown in Eq. (12). On the other hand, HL-LHC can probe κ_Z to $\sim 2\%$ precision via $h \to ZZ^* \to 4\ell$ decays and ILC can probe to sub-percent precision since h is dominantly produced via Higgsstrahlung: $e^+e^- \to Z^* \to Zh$. Even so, the bulk of points with low $\Delta_{\rm EW}$ have only tiny deviations from 1 and so in this channel one expects the h to look highly SM-like for RNS SUSY.

As we have discussed so far, the deviations in the fermion and gauge boson couplings are mainly due to the effects of a sizable $\cos(\alpha+\beta)$, which occurs if m_A is relatively light. Such effects are, however, also induced in the two-Higgs doublet models. To confirm the presence of SUSY effects, therefore, it is desirable to see the contribution given by other particles than the Higgs bosons. To that end, we consider the following quantity discussed in Ref. [53]:

$$\frac{\kappa_b - \kappa_\tau}{\kappa_t - \kappa_b} \simeq \Delta_b \ , \tag{30}$$

where we have kept only the $\tan\beta$-enhanced terms and used the fact that $|\Delta_\tau|$ is rather small since it is induced by the electroweak gaugino loop diagrams. In Fig. 6, we plot this quantity vs. $\Delta_{\rm EW}$ with color coding in accord with $m_{\tilde{t}_1}$. It is found that a sizable value of Δ_b is

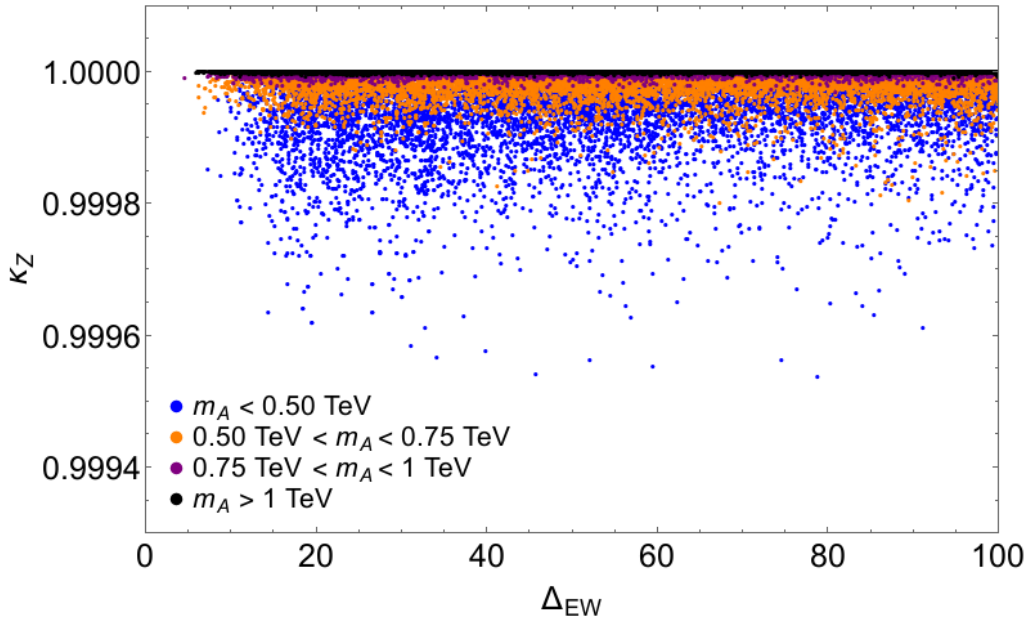

Figure 5: κ_Z vs. $\Delta_{\rm EW}$ from scan over NUHM2 parameter space with $m_h = 125 \pm 2$ GeV and LHC Higgs and sparticle mass constraints.

expected in most of parameter points. Therefore, we may extract even the information of the sfermion/gaugino sector via the precise measurements of the fermion couplings. However, we also note that the value of the quantity is found to be relatively small in the small $\Delta_{\rm EW}$ region. This challenges the extraction of Δ_b in the natural SUSY scenario.

In Fig. 7, we show the value of κ_g vs. $\Delta_{\rm EW}$. In this plot, the dots are color coded as to the value of $m_{\tilde{t}_1}$, with blue indicating $m_{\tilde{t}_1} < 1.5$ TeV, yellow is 1.5 TeV $< m_{\tilde{t}_1} < 3$ TeV, green is 3 TeV$< m_{\tilde{t}_1} < 4$ TeV and red is $m_{\tilde{t}_1} > 4$ TeV. Here, the hgg coupling proceeds from triangle diagrams including quarks for the SM case and also squarks for the SUSY case. Thus, we expect large deviations from the SM coupling if squarks are far lighter than the TeV range. Since we require $m_h \sim 125$ GeV, then we implicitly require TeV-scale highly mixed top squarks which provide a sufficiently large radiative correction to m_h. Usually the top squarks are amongst the lightest squarks since their masses are suppressed by large top-quark Yukawa effects in RG running, and also by large mixing. Furthermore, the NUHM2 model should obey well the LHC8 constraints on the minimal SUGRA model (mSUGRA) [6, 7] so that $m_{\tilde{q}} \gtrsim 1.8$ TeV. Thus, we do not expect squarks well below the TeV-scale and therefore large deviations in the κ_g coupling. While some points with low $m_{\tilde{t}_1}$ have deviations of several %, which can be probed by HL-LHC via the overall s-channel Higgs production rate $\sigma(gg \to h)$, the bulk of points with a decoupled $m_{\tilde{t}_1}$ in the TeV-range tend to have deviations of less than a percent. These deviations will be hard to access by either HL-LHC or by ILC. Note that most of the parameter points predict $\kappa_g < 1$. As discussed above, this can happen only when there exists a large left-right mixing in the stop mass matrix. Since this large mixing is a typical feature of the RNS models, the reduction in the hgg coupling can be regarded as a distinctive prediction in the RNS scenario.

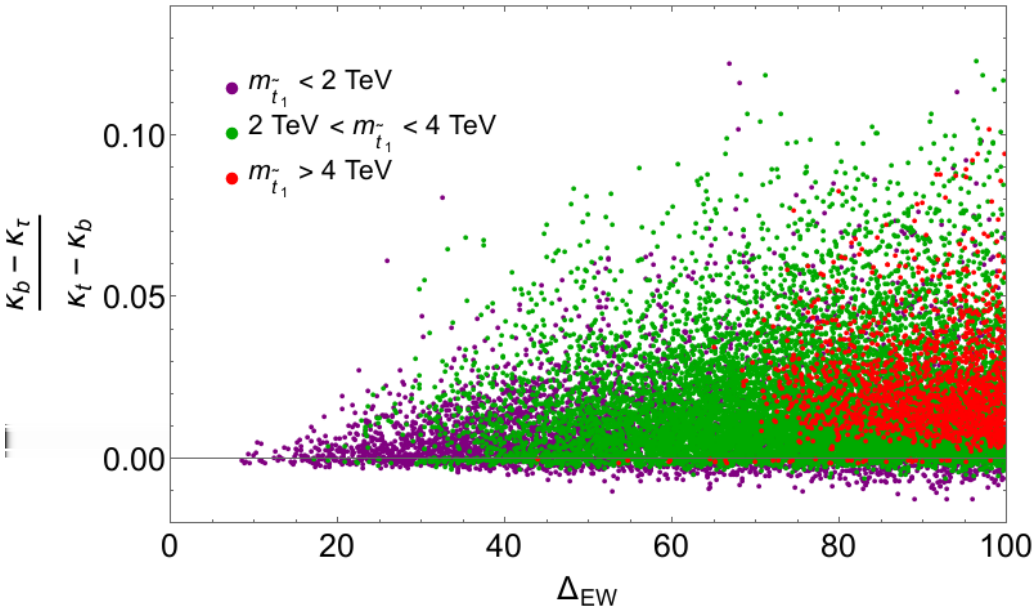

Figure 6: $(\kappa_b - \kappa_\tau)/(\kappa_t - \kappa_b)$ vs. $\Delta_{\rm EW}$ from scan over NUHM2 parameter space with $m_h = 125 \pm 2$ GeV and LHC Higgs and sparticle mass constraints.

In Fig. 8, we show the value of κ_γ vs. $\Delta_{\rm EW}$. Color coding is the same as in Fig. 7. In the SM, the κ_γ coupling proceeds via triangle diagrams involving charged particles which couple to the Higgs: the qs, ℓs and $W^\pm$. Among them, top quark and W boson give rise to the dominant contributions. In the case of SUSY, then there are additional loops containing squarks, sleptons, charginos and charged Higgs bosons. As in the case of κ_g, large deviations are obtained in the light stop region which also coincides with the small μ region (with light charginos). Moreover, for $m_{H^\pm} \sim m_A$ small (large Higgs mixing) then the hH^+H^- coupling can lead to deviations in κ_γ as in two Higgs doublet models. For light charginos, then the $h\widetilde{W}_1\widetilde{W}_1$ coupling can be large and also contribute. This coupling is proportional to higgsino-times-gaugino components of $\widetilde{W}_1$ and so in the case where $\widetilde{W}_1$ is nearly pure higgsino or wino, the coupling is smaller. From the plot, we expect deviations in $\kappa_\gamma \lesssim 1\%$.

Even though the $h \to \gamma\gamma$ branching fraction is small, the LHC $gg \to h$ production cross section is large and the $\gamma\gamma$ signature is robust. For comparison, the reach in κ_γ of HL-LHC is shown which extends to the 2% level. This is not enough to access the bulk of low fine-tuned RNS models. The small $h \to \gamma\gamma$ branching fraction limits the ILC capability to probe this loop-induced coupling. ILC500 is projected to probe values of κ_γ to the 8% level. [17]

6 Natural SUSY with light wino

The results from the previous Section were evaluated in the NUHM2 model which assumes gaugino mass unification: $M_1 = M_2 = M_3$ at the GUT scale so that $M_3 \sim 7M_1$ and $M_2 \sim 2M_1$ at the weak scale due to RG evolution. Then the LHC limit (that $m_{\tilde{g}} \gtrsim 1.3$ TeV from the

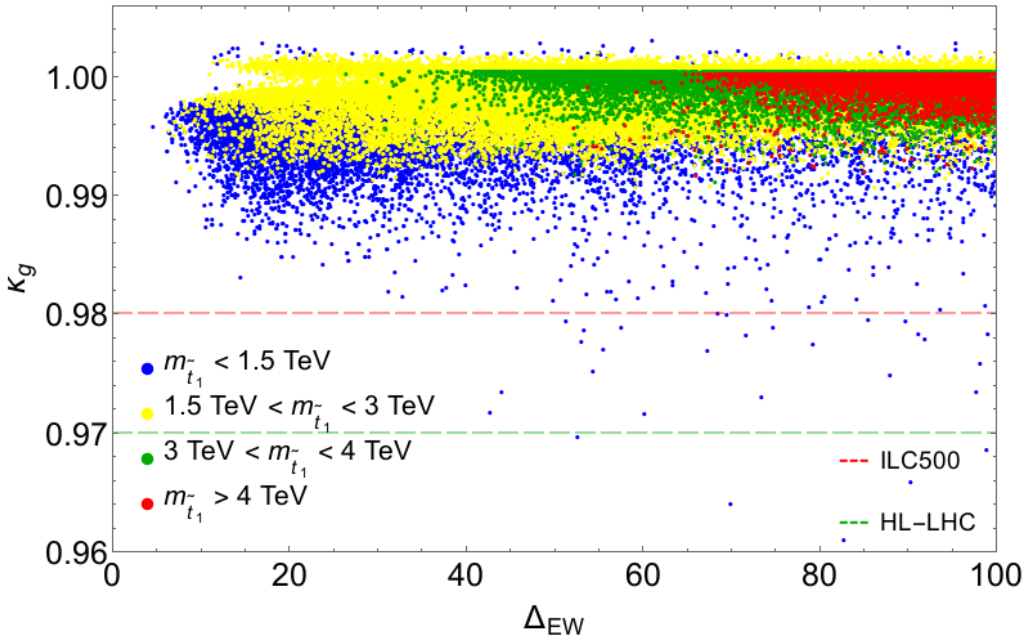

Figure 7: κ_g vs. $\Delta_{\rm EW}$ from scan over NUHM2 parameter space with $m_h = 125 \pm 2$ GeV and LHC Higgs and sparticle mass constraints.

mSUGRA cascade decay analysis) translates roughly to $M_2 \gtrsim 350$ GeV and $M_1 \gtrsim 175$ GeV. This means for RNS SUSY with low $\mu \sim 100 - 200$ GeV that the light $\widetilde{W}_1$ which circulates in the $h\gamma\gamma$ loop is mainly higgsino-like and has somewhat suppressed couplings. The $h\gamma\gamma$ coupling can be increased in models with non-universal gaugino masses where $m_{\tilde{g}}$ can remain above the LHC8 bound, but now M_2 and M_1 can be much lower resulting in natural SUSY with either a wino-like or bino-like LSP [38].

In the RNS case with non-universal gaugino masses and a lower value of M_2, then the $\widetilde{W}_1$ can be a wino-higgsino admixture. Such a mixed chargino enhances its coupling to the Higgs boson[11] h which depends on a product of gaugino times higgsino components.

To show a case with maximal κ_γ in RNS, we plot in Fig. 9 the value of κ_γ vs. M_2 along an RNS model-line with parameters $m_0 = 5$ TeV, $m_{1/2} = 0.7$ TeV, $A_0 = -8$ TeV, $\mu = 200$ GeV and $m_A = 1$ TeV. We abandon gaugino mass unification and instead allow M_2 to vary. We also plot results for several $\tan\beta$ values. For the case shown, as M_2 decreases from its universal value, the $\widetilde{W}_1$ becomes more of a mixed wino-higgsino state and the coupling $h\widetilde{W}_1\widetilde{W}_1$ increases. Correspondingly, κ_γ increases. The maximal κ_γ reaches ~ 1.03 for lower values of $\tan\beta$ and for $M_2 \sim 150$ GeV with $\Delta_{\rm EW} \sim 10$. Such a large value of κ_γ should be accessible to HL-LHC as shown by the green dashed line. Larger values of $\tan\beta \gtrsim 40$ ($\Delta_{\rm EW} \sim 50$) are excluded by $B_s \to \mu^+\mu^-$ constraint since $\mathrm{Br}(B_s \to \mu^+\mu^-) \propto \tan^6\beta$ as stated in Eq. (27).

It is also interesting to see that negative μ makes κ_γ smaller than unity. If stops are as heavy as a few TeV, which is required to obtain the 125 GeV Higgs mass, main contributions to Higgs-to-diphoton decay come from chargino loops, so $\kappa_\gamma < 1$ means that chargino loop

[11] See p. 178 of Ref. [40].

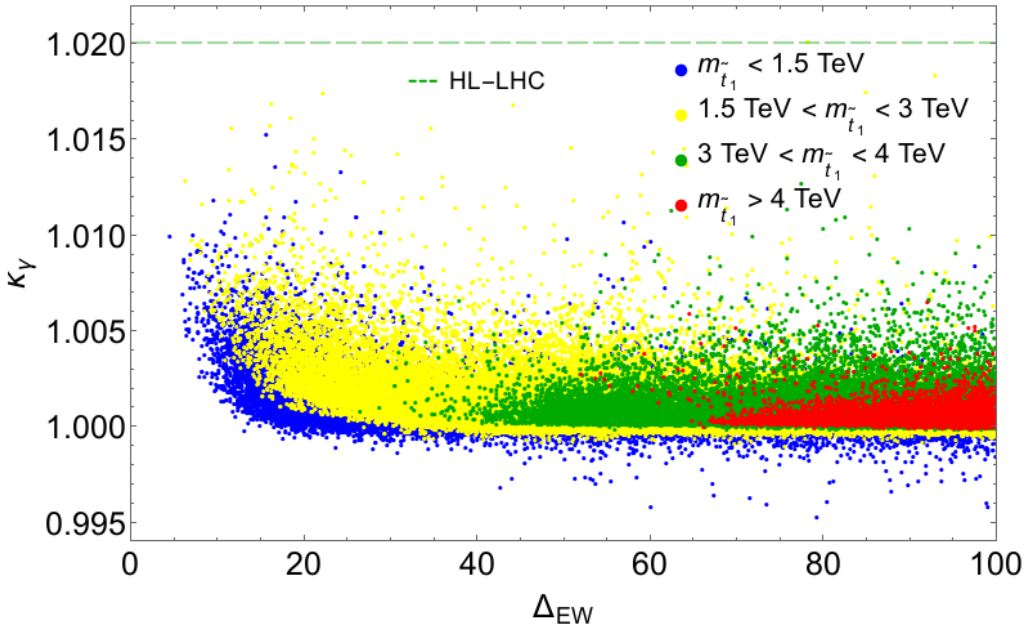

Figure 8: κ_γ vs. $\Delta_{\rm EW}$ from scan over NUHM2 parameter space with $m_h = 125 \pm 2$ GeV and LHC Higgs and sparticle mass constraints.

contributions destructively interfere the dominant W boson loop contribution. It is simply understood from the $h\widetilde{W}\widetilde{W}$ coupling, which is given by[12]

$$g_{h\widetilde{W}_1\widetilde{W}_1} \simeq g_2 \ \mathrm{sign}(\mu) \left| \frac{m_W^2(M_2 \cos\beta + \mu \sin\beta)}{M_2^2 - \mu^2} \right|, \tag{31}$$

$$g_{h\widetilde{W}_2\widetilde{W}_2} \simeq g_2 \ \mathrm{sign}(\mu) \left| \frac{m_W^2(M_2 \sin\beta + \mu \cos\beta)}{M_2^2 - \mu^2} \right|, \tag{32}$$

where $m_A^2 \gg m_h^2$, $|M_2^2 - \mu^2| \gg m_W^2$ and $|M_2/\mu| < \tan\beta$. Here we assume that $\widetilde{W}_1$ is mostly higgsino-like and $\widetilde{W}_2$ is mostly wino-like. The chargino-Higgs couplings flip their sign when the sign of μ is flipped, and thus chargino contributions can be either constructive and destructive depending on the sign of μ. In order to avoid chargino LSP, for $\mu < 0$ we set $M_1 = 100$ GeV. κ_γ can show about 2% deficit for small $\tan\beta$ and M_2, and it approaches to the SM value as M_2 increases (black curve).

If a deviation in κ_γ is actually observed at the LHC, this may indicate the presence of a light chargino with sizable coupling to the Higgs boson. Such a light chargino should be within the reach of direct production at the ILC. Moreover, a large coupling to the Higgs boson implies a large neutralino-nucleon scattering cross section. Although we expect that only a small portion of dark matter energy density is occupied by the $\widetilde{Z}_1$ LSP since such a light higgsino-like neutralino in general results in a small relic abundance, it is found that future dark matter direct detection experiments can probe the $\widetilde{Z}_1$ LSP in this case, and thus provide a way of examining RNS models [69].

[12] See Sec. 8.3 and 8.4 of Ref. [40] for complete formulae.

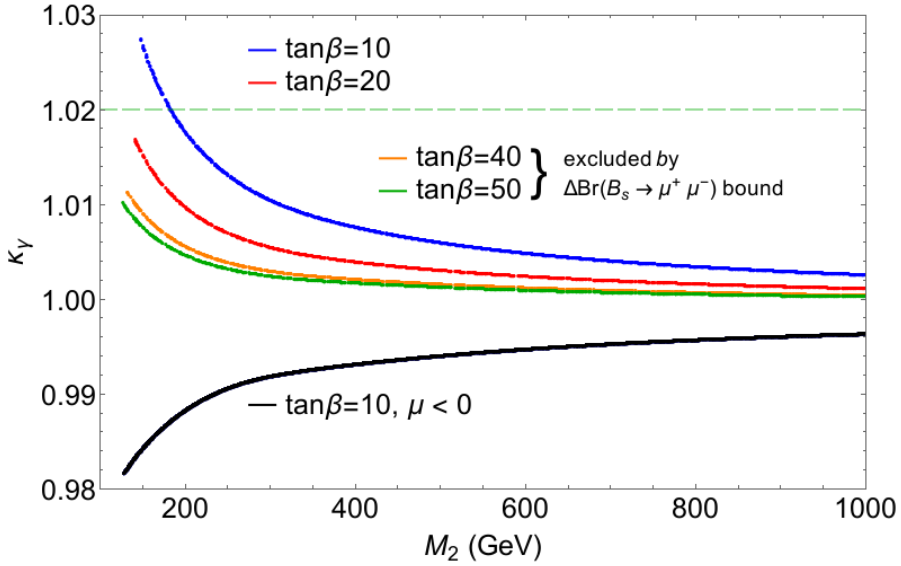

Figure 9: κ_γ vs. M_2 along the RNS model line for various values of $\tan\beta$. The reach of HL-LHC is shown by the green dashed line.

7 Conclusions:

In this paper we have presented expectations for possible deviations in Higgs couplings that are expected in SUSY models with radiatively-driven naturalness. Such models with low $\Delta_{\rm EW} \lesssim 30$ are natural in the electroweak sector and, if augmented with a Peccei-Quinn sector, are natural in the QCD sector as well. Models with a SUSY DFSZ axion also admit an elegant solution to the SUSY μ problem. Such natural SUSY models are consistent with squark, slepton and gravitino masses in the multi-TeV range which admits a solution to the gravitino problem [70,71] and at least a partial decoupling solution to the SUSY flavor and CP problems [72]. These models are rather simple extensions of the SM and may even be regarded as more conservative than the SM in that they contain solutions to the gauge hierarchy and strong CP problems. Thus, every avenue for their verification must be explored. Here, we examined the case of Higgs boson profiling.

Our results may be summarized as follows.

- Substantial deviations in κ_τ and κ_b may be expected for RNS SUSY but mainly in the case where m_A is rather light leading to significant mixing in the scalar Higgs sector. However, since m_A can extend into the multi-TeV range at little cost to naturalness (due to $\tan^2\beta$ suppression of the term including $m^2_{H_d}$ in Eq. (1)) these deviations may well lie below the reach of HL-LHC and even ILC500.

- Tiny deviations to κ_t are expected. This coupling is also difficult to measure unless one has a linear e^+e^- collider with $\sqrt{s} > m_h + 2m_t$.

- Tiny deviations are expected in $\kappa_{W,Z}$, usually below the 0.5% level.

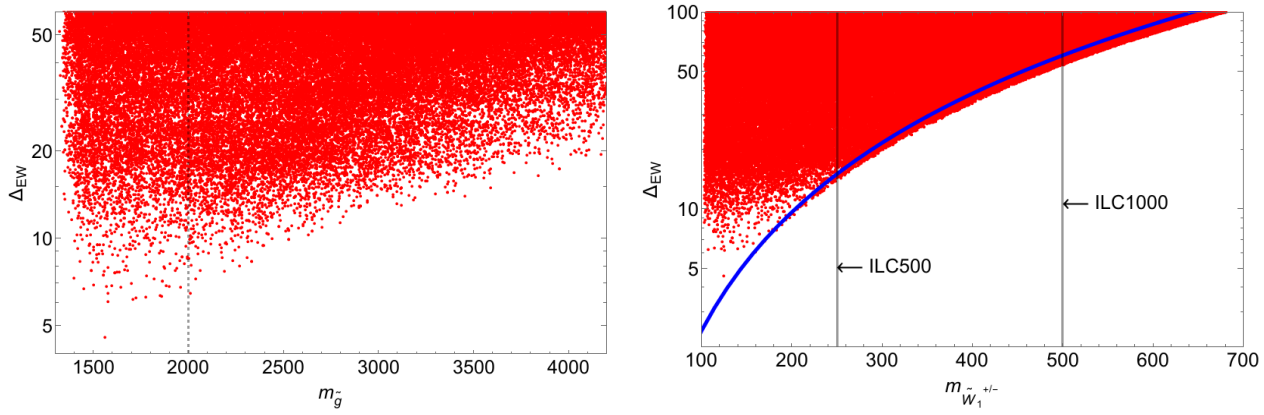

(a) (b)

Figure 10: (a) Plot of $\Delta_{\rm EW}$ vs. $m_{\tilde{g}}$ from a scan over NUHM2 parameter space. (b) Plot of $\Delta_{\rm EW}$ vs. $m_{\widetilde{W}_1}$ from a scan over NUHM2 parameter space. We also show the curve $\Delta_{\rm EW}=\mu^2/(m_Z^2/2)$ and the reach of various ILC energy options for higgsino pair production.

- Some deviations can occur in the κ_g coupling, but mainly for anomalous cases with very light top squarks $\tilde{t}_1$. However, light top squarks generally lead to large deviations in $BF(b\rightarrow s\gamma)$ and also have recently been tightly constrained by top-squark pair production searches at LHC8 [73, 74]. Except for such cases, most RNS predictions for κ_g lie below the reach of HL-LHC and ILC500.

- Small deviations in κ_γ are expected– usually at the sub-0.5% level– below the reach of HL-LHC and ILC500. However, in models with non-universal gaugino masses where the light chargino becomes a wino-higgsino mixture, then κ_γ may increase to the 1–3% level.

To summarize: except for unusual cases (highly mixed Higgs sector with low m_A, anomalously light stops soon to be excluded by LHC or highly mixed charginos) natural SUSY predicts minimal deviations from a SM-like portrait of the light Higgs boson. Given this situation, it is useful to compare these indirect search methods against the direct search for natural SUSY at LHC and ILC.

A direct search for $\tilde{g}\tilde{g}$ production at LHC13 with 1000 fb^{-1} can reach up to $m_{\tilde{g}}\sim 2$ TeV [10]. This approximately covers $\Delta_{\rm EW}<7$ as seen in Fig. 10(a). The LHC13 1000 fb^{-1} reach for $\tilde{g}\tilde{g}$ production is also shown in terms of $\Delta_{\rm EW}$ by the brown histogram of Fig. 11. LHC13 can also search for light higgsino pair production $pp\rightarrow\widetilde{Z}_1\widetilde{Z}_2$ where $\widetilde{Z}_2\rightarrow\mu^+\mu^-\widetilde{Z}_1$. Since the dimuons tend to be rather soft (due to the small $m_{\widetilde{Z}_2}-m_{\widetilde{Z}_1}$ mass gap) a trigger on hard jet radiation from the initial state is needed [13]. The reach of various LHC13 options for $\mu^+\mu^-j+E_T^{\rm miss}$ production is also shown in Fig. 11.

The most direct test of SUSY naturalness occurs via the direct search for higgsino pair production at an e^+e^- collider with $\sqrt{s}>2\mu$. Such a machine would be a higgsino factory [39] in addition to a Higgs factory. The value of $m_{\widetilde{W}_1}$ is plotted versus $\Delta_{\rm EW}$ in Fig. 10(b) which exhibits the tight correlation where $\sqrt{s}>2m_{\widetilde{W}_1}$ and where $m_{\widetilde{W}_1}\simeq\mu$. Since $\Delta_{\rm EW}\sim\mu^2/(m_Z^2/2)$, then ILC probes directly values of $\Delta_{\rm EW}$ according to $\sqrt{s}\sim\sqrt{2\Delta_{\rm EW}}m_Z$. From the plot, we see

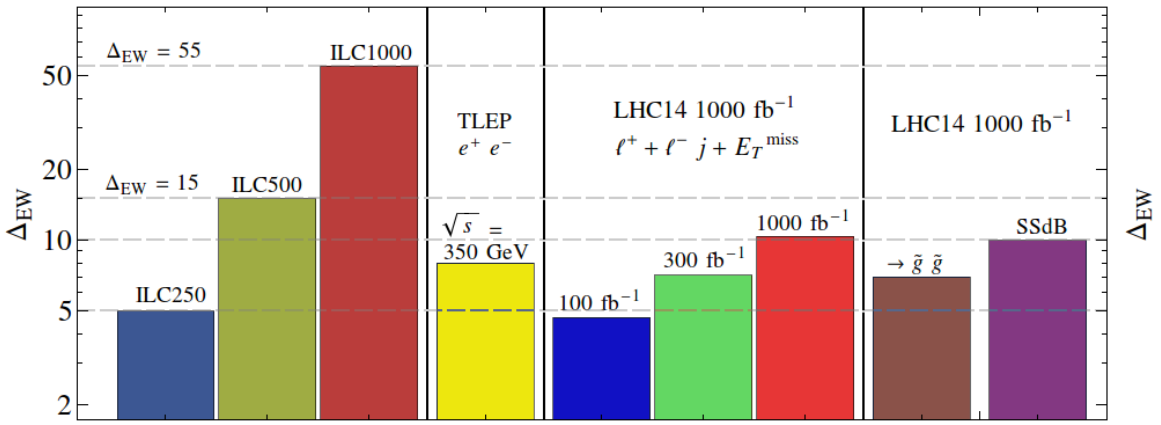

Figure 11: Plot of the reach of various LHC and ILC options for SUSY with radiatively-driven naturalness in terms of $\Delta_{\rm EW}$.

that ILC500 makes a complete probe of $\Delta_{\rm EW} < 15$ and ILC1000 probes $\Delta_{\rm EW} < 55$.

In Fig. 11, we show the reach in $\Delta_{\rm EW}$ of prospective experiments. ILC1000 can see the entire RNS parameter space whereas LHC14 and TLEP can probe only a portion of it. Light higgsinos should ultimately be detected at ILC with $\sqrt{s} > 2\mu$.

Acknowledgments

This work was supported in part by the US Department of Energy, Office of High Energy Physics. The work of NN is supported by Research Fellowships of the Japan Society for the Promotion of Science for Young Scientists. KJB, HB and HS would like to thank the William I. Fine Institute for Theoretical Physics (FTPI) at the University of Minnesota for hospitality while this work was initiated. The computing for this project was performed at the OU Supercomputing Center for Education & Research (OSCER) at the University of Oklahoma (OU).

References

[1] G. Aad *et al.* [ATLAS Collaboration], *Phys. Lett.* **B 716** (2012) 1.

[2] S. Chatrchyan *et al.* [CMS Collaboration], *Phys. Lett.* **B 716** (2012) 30.

[3] G. Aad *et al.* [ATLAS and CMS Collaborations], arXiv:1503.07589 [hep-ex].

[4] L. Susskind, Phys. Rev. D **20** (1979) 2619.

[5] E. Witten, Nucl. Phys. B **188**, 513 (1981); R. K. Kaul, Phys. Lett. B **109**, 19 (1982).

[6] G. Aad *et al.* [ATLAS Collaboration], *J. High Energy Phys.* **1409** (2013) 176.

[7] S. Chatrchyan *et al.* [CMS Collaboration], *J. High Energy Phys.* **1406** (2014) 055.

[8] H. Baer, V. Barger, P. Huang, A. Mustafayev and X. Tata, Phys. Rev. Lett. **109** (2012) 161802; H. Baer, V. Barger, P. Huang, D. Mickelson, A. Mustafayev and X. Tata, Phys. Rev. D **87** (2013) 115028.

[9] H. Baer, V. Barger, A. Lessa and X. Tata, Phys. Rev. D **86** (2012) 117701.

[10] H. Baer, V. Barger, P. Huang, D. Mickelson, A. Mustafayev, W. Sreethawong and X. Tata, JHEP **1312** (2013) 013.

[11] H. Baer, V. Barger, P. Huang, D. Mickelson, A. Mustafayev, W. Sreethawong and X. Tata, Phys. Rev. Lett. **110** (2013) 151801.

[12] C. Han, A. Kobakhidze, N. Liu, A. Saavedra, L. Wu and J. M. Yang, *J. High Energy Phys.* **1402** (2014) 049; H. Baer, A. Mustafayev and X. Tata, *Phys. Rev.* **D 89** (2014) 055007; D. Barducci, A. Belyaev, A. K. M. Bharucha, W. Porod and V. Sanz, arXiv:1504.02472 [hep-ph].

[13] Z. Han, G. D. Kribs, A. Martin and A. Menon, Phys. Rev. D **89** (2014) 075007; H. Baer, A. Mustafayev and X. Tata, Phys. Rev. D **90** (2014) 115007.

[14] V. Khachatryan *et al.* [CMS Collaboration], arXiv:1411.3441 [hep-ex]; The ATLAS collaboration, ATLAS-CONF-2015-008.

[15] T. Han, Z. Liu and J. Sayre, Phys. Rev. D **89** (2014) 113006 [arXiv:1311.7155 [hep-ph]].

[16] M. E. Peskin, arXiv:1312.4974 [hep-ph].

[17] S. Dawson, A. Gritsan, H. Logan, J. Qian, C. Tully, R. Van Kooten, A. Ajaib and A. Anastassov *et al.*, arXiv:1310.8361 [hep-ex].

[18] G. Moortgat-Pick, H. Baer, M. Battaglia, G. Belanger, K. Fujii, J. Kalinowski, S. Heinemeyer and Y. Kiyo *et al.*, arXiv:1504.01726 [hep-ph].

[19] M. Carena, S. Gori, N. R. Shah and C. E. M. Wagner, JHEP **1203** (2012) 014 [arXiv:1112.3336 [hep-ph]]; M. Carena, S. Gori, N. R. Shah, C. E. M. Wagner and L. T. Wang, JHEP **1207** (2012) 175 [arXiv:1205.5842 [hep-ph]]; M. Carena, S. Gori, I. Low, N. R. Shah and C. E. M. Wagner, JHEP **1302** (2013) 114 [arXiv:1211.6136 [hep-ph]]; M. Carena, S. Gori, N. R. Shah, C. E. M. Wagner and L. T. Wang, JHEP **1308** (2013) 087.

[20] N. Arkani-Hamed, K. Blum, R. T. D'Agnolo and J. Fan, JHEP **1301** (2013) 149 [arXiv:1207.4482 [hep-ph]].

[21] A. Djouadi, Eur. Phys. J. C **74** (2014) 2704 [arXiv:1311.0720 [hep-ph]].

[22] M. Cahill-Rowley, J. Hewett, A. Ismail and T. Rizzo, Phys. Rev. D **90** (2014) 095017 [arXiv:1407.7021 [hep-ph]].

[23] M. Endo, T. Moroi and M. M. Nojiri, arXiv:1502.03959 [hep-ph].

[24] B. Bhattacherjee, A. Chakraborty and A. Choudhury, arXiv:1504.04308 [hep-ph].

[25] G. D. Kribs, A. Martin and A. Menon, Phys. Rev. D **88** (2013) 035025 [arXiv:1305.1313 [hep-ph]].

[26] J. Fan and M. Reece, JHEP **1406** (2014) 031 [arXiv:1401.7671 [hep-ph]].

[27] T. Gherghetta, B. von Harling, A. D. Medina and M. A. Schmidt, JHEP **1404** (2014) 180.

[28] B. Henning, X. Lu and H. Murayama, arXiv:1404.1058 [hep-ph].

[29] J. Fan, M. Reece and L. T. Wang, arXiv:1412.3107 [hep-ph].

[30] H. Baer, V. Barger and D. Mickelson, Phys. Rev. D **88** (2013) 095013.

[31] H. Baer, V. Barger, D. Mickelson and M. Padeffke-Kirkland, Phys. Rev. D **89** (2014) 115019.

[32] R. D. Peccei and H. R. Quinn, Phys. Rev. Lett. **38**, 1440 (1977); S. Weinberg, Phys. Rev. Lett. **40**, 223 (1978); F. Wilczek, Phys. Rev. Lett. **40**, 279 (1978).

[33] M. Dine, W. Fischler and M. Srednicki, Phys. Lett. B **104**, 199 (1981); A. R. Zhitnitsky, Sov. J. Nucl. Phys. **31**, 260 (1980) [Yad. Fiz. **31**, 497 (1980)].

[34] H. Murayama, H. Suzuki and T. Yanagida, Phys. Lett. B **291** (1992) 418.

[35] K. J. Bae, H. Baer and H. Serce, Phys. Rev. D **91** (2015) 015003 [arXiv:1410.7500 [hep-ph]].

[36] N. Craig, arXiv:1309.0528 [hep-ph].

[37] D. Matalliotakis and H. P. Nilles, Nucl. Phys. B **435** (1995) 115; P. Nath and R. L. Arnowitt, Phys. Rev. D **56** (1997) 2820; J. Ellis, K. Olive and Y. Santoso, Phys. Lett. **B539** (2002) 107; J. Ellis, T. Falk, K. Olive and Y. Santoso, Nucl. Phys. **B652** (2003) 259; H. Baer, A. Mustafayev, S. Profumo, A. Belyaev and X. Tata, JHEP**0507** (2005) 065.

[38] H. Baer, V. Barger, P. Huang, D. Mickelson, M. Padeffke-Kirkland and X. Tata, Phys. Rev. D **91** (2015) 075005 [arXiv:1501.06357 [hep-ph]].

[39] H. Baer, V. Barger, D. Mickelson, A. Mustafayev and X. Tata, JHEP **1406** (2014) 172.

[40] H. Baer and X. Tata, *Weak Scale Supersymmetry: From Superfields to Scattering Events*, (Cambridge University Press, 2006).

[41] A. Mustafayev and X. Tata, Indian J. Phys. **88** (2014) 991;

[42] K. Chan, U. Chattopadhyay and P. Nath, *Phys. Rev.* **D 58** (1998) 096004.

[43] H. Baer, V. Barger, P. Huang, D. Mickelson, A. Mustafayev and X. Tata, Phys. Rev. D **87** (2013) 035017 [arXiv:1210.3019 [hep-ph]].

[44] R. Harnik, G. D. Kribs, D. T. Larson and H. Murayama, Phys. Rev. D **70** (2004) 015002 [hep-ph/0311349].

[45] R. Kitano and Y. Nomura, Phys. Lett. B **631**, 58 (2005) [hep-ph/0509039]; R. Kitano and Y. Nomura, Phys. Rev. D **73**, 095004 (2006) [hep-ph/0602096].

[46] M. Papucci, J. T. Ruderman and A. Weiler, JHEP **1209** (2012) 035.

[47] L. J. Hall, D. Pinner and J. T. Ruderman, JHEP **1204** (2012) 131.

[48] H. Baer, V. Barger and M. Savoy, Phys. Scripta **90** (2015) 6, 068003 [arXiv:1502.04127 [hep-ph]].

[49] J. R. Ellis, K. Enqvist, D. V. Nanopoulos and F. Zwirner, Mod. Phys. Lett. A **1** (1986) 57.

[50] R. Barbieri and G. Giudice, *Nucl. Phys.* **B 306** (1988) 63.

[51] For reviews, see J. L. Feng, Ann. Rev. Nucl. Part. Sci. **63** (2013) 351 and G. G. Ross, Eur. Phys. J. C **74** (2014) 2699.

[52] S. K. Soni and H. A. Weldon, Phys. Lett. B **126** (1983) 215; V. S. Kaplunovsky and J. Louis, Phys. Lett. B **306** (1993) 269; A. Brignole, L. E. Ibanez and C. Munoz, Nucl. Phys. B **422** (1994) 125 [Erratum-ibid. B **436** (1995) 747].

[53] M. Carena, H. E. Haber, H. E. Logan and S. Mrenna, Phys. Rev. D **65**, 055005 (2002) [Phys. Rev. D **65**, 099902 (2002)] [hep-ph/0106116].

[54] W. Siegel, Phys. Lett. B **84**, 193 (1979).

[55] L. J. Hall, R. Rattazzi and U. Sarid, Phys. Rev. D **50** (1994) 7048; R. Hempfling, Phys. Rev. D **49** (1994) 6168; M. Carena, M. Olechowski, S. Pokorski and C. E. M. Wagner, Nucl. Phys. B **426** (1994) 269; M. Carena, S. Mrenna and C. E. M. Wagner, Phys. Rev. D **60** (1999) 075010.

[56] D. M. Pierce, J. A. Bagger, K. T. Matchev and R. j. Zhang, Nucl. Phys. B **491**, 3 (1997) [hep-ph/9606211].

[57] J. Guasch, W. Hollik and S. Penaranda, Phys. Lett. B **515**, 367 (2001) [hep-ph/0106027].

[58] P. Kalyniak, R. Bates and J. N. Ng, Phys. Rev. D **33** (1986) 755; R. Bates, J. N. Ng and P. Kalyniak, Phys. Rev. D **34** (1986) 172; J. F. Gunion, G. Gamberini and S. F. Novaes, Phys. Rev. D **38** (1988) 3481; J. F. Gunion, H. E. Haber, G. L. Kane and S. Dawson, Front. Phys. **80** (2000) 1; we use Isajet evaluations as given in M. A. Bisset, UMI-95-32579.

[59] A. Arvanitaki and G. Villadoro, JHEP **1202**, 144 (2012) [arXiv:1112.4835 [hep-ph]]; D. Carmi, A. Falkowski, E. Kuflik and T. Volansky, JHEP **1207**, 136 (2012) [arXiv:1202.3144 [hep-ph]]; K. Blum, R. T. D'Agnolo and J. Fan, JHEP **1301**, 057 (2013) [arXiv:1206.5303 [hep-ph]].

[60] H. Baer and M. Brhlik, Phys. Rev. D **55** (1997) 3201; H. Baer, M. Brhlik, D. Castano and X. Tata, Phys. Rev. D **58** (1998) 015007.

[61] M. Carena, D. Garcia, U. Nierste and C. E. M. Wagner, Phys. Lett. B **499**, 141 (2001) [hep-ph/0010003].

[62] J. K. Mizukoshi, X. Tata and Y. Wang, Phys. Rev. D **66** (2002) 115003.

[63] G. Aad *et al.* [ATLAS Collaboration], JHEP **1411** (2014) 056.

[64] V. Khachatryan *et al.* [CMS Collaboration], JHEP **1410** (2014) 160.

[65] K. J. Bae, H. Baer, V. Barger, D. Mickelson and M. Savoy, Phys. Rev. D **90** (2014) 075010 [arXiv:1407.3853 [hep-ph]].

[66] V. D. Barger, H. Baer and K. Hagiwara, Phys. Lett. B **146** (1984) 257.

[67] ISAJET, by H. Baer, F. Paige, S. Protopopescu and X. Tata, hep-ph/0312045.

[68] Joint LEP 2 Supersymmetry Working Group, *Combined LEP Chargino Results up to 208 GeV*, `http://lepsusy.web.cern.ch/lepsusy/www/inos_moriond01/charginos_pub.html`.

[69] H. Baer, V. Barger and D. Mickelson, Phys. Lett. B **726** (2013) 330; K. J. Bae, H. Baer, V. Barger, M. R. Savoy and H. Serce, arXiv:1503.04137 [hep-ph].

[70] S. Weinberg, Phys. Rev. Lett. **48**, 1303 (1982).

[71] M. Kawasaki, K. Kohri, T. Moroi and A. Yotsuyanagi, Phys. Rev. D **78**, 065011 (2008) [arXiv:0804.3745 [hep-ph]].

[72] F. Gabbiani, E. Gabrielli, A. Masiero and L. Silvestrini, Nucl. Phys. B **477**, 321 (1996) [hep-ph/9604387].

[73] G. Aad *et al.* [ATLAS Collaboration], JHEP **1411**, 118 (2014) [arXiv:1407.0583 [hep-ex]].

[74] CMS Collaboration [CMS Collaboration], CMS-PAS-SUS-14-011.